

Diffusion-Reinforcement Learning Hierarchical Motion Planning in Adversarial Multi-agent Games

Zixuan Wu*, Sean Ye*, Manisha Natarajan* and Matthew C. Gombolay*

Abstract—Reinforcement Learning- (RL-)based motion planning has recently shown the potential to outperform traditional approaches from autonomous navigation to robot manipulation. In this work, we focus on a motion planning task for an evasive target in a partially observable multi-agent adversarial pursuit-evasion games (PEG). These pursuit-evasion problems are relevant to various applications, such as search and rescue operations and surveillance robots, where robots must effectively plan their actions to gather intelligence or accomplish mission tasks while avoiding detection or capture themselves. We propose a hierarchical architecture that integrates a high-level diffusion model to plan global paths responsive to environment data while a low-level RL algorithm reasons about evasive versus global path-following behavior. Our approach outperforms baselines by 51.2% by leveraging the diffusion model to guide the RL algorithm for more efficient exploration and improves the explainability and predictability.¹

I. INTRODUCTION

Multi-agent pursuit-evasion games (PEG) [1] are ubiquitous in real-world robotics scenarios where robotic systems could be applied to tracking drug smugglers [2], defensive escorting [3], or robot soccer [4]. In PEG, one team seeks to track its target while the target agent or team employs evasive maneuvers, and research naturally focuses on developing methods for either the pursuers [5] or evaders [6]–[8]. While there has been extensive work on developing search policies, including robust tracking frameworks [9], topology map maintenance [10], and multi-hypothesis filters [11], relatively little attention has been paid to evasion. This lack of emphasis provides an opportunity to design a novel evasive policy which is also useful in the real-world scenarios (e.g. business ship evading from pirates).

Traditional approaches to develop evasion policies typically assume full environment observability and are designed to optimize capture time [12] or an ad hoc utility function [13]. More recently, learning-based methods, such as Graph Neural Networks [14], diffusion models [15] or reinforcement learning (RL) methods [16] have been widely used in the pursuit-evasion games and in similar navigation problems [17]–[19] (e.g. goal-reaching, path-planning, etc.). These methods often outperform expert policies [20]. Unfortunately, learning the RL policy is usually subject to two key challenges—partial observability and high sample complexity when exploring in large-scale, partially observable

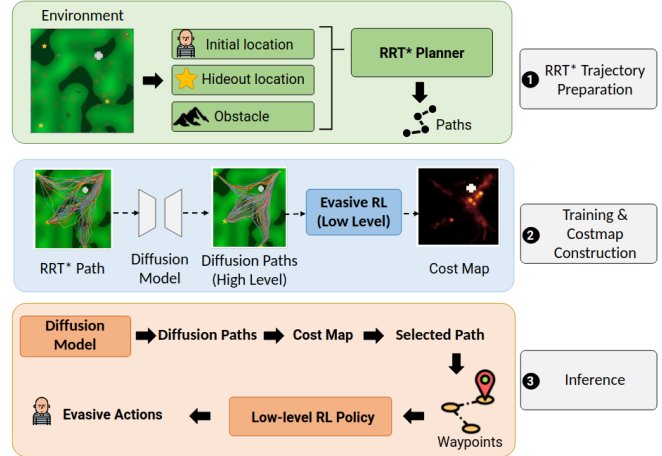


Fig. 1. Diffusion-RL framework overview: We first collect RRT* paths into a dataset. Then we use a diffusion model to learn the distribution of the RRT* path and generate samples as the high-level global plans to help learn a low-level evasive RL policy. A posterior costmap is built based on the learned hierarchy and detection risk and can be used to select the best global path in the inference stage.

environments, as considered in our work.

Researchers propose hierarchical approaches to help exploration by structuring the goal, policies, or rewards. Goal-oriented reinforcement learning (e.g. hindsight experience replay [21]) increases the reward density by assuming the goal has been reached in each exploration trajectory and correcting observation and reward accordingly. Hierarchical reinforcement learning [22] improves the sample efficiency from spatial or temporal abstraction by multiple hierarchically organized RL policies, and hybrid reward structure based methods [23] try to capture the multi-modal distribution of reward where each part of value function can be a low-dimensional representation. However, their applications are either tested in fully observable games [22] or single agent scenarios [24], and sometimes require expert prior knowledge as primitives [25].

In this paper, we propose a novel hierarchical learning framework that utilizes diffusion and RL as high and low level policies respectively. The diffusion model is used as a global path generator to satisfy static map constraints, such as terminal states and obstacle avoidance. Additionally, we employ a low-level RL policy that learns to follow the waypoints while prudently evading captures (see Figure 1). Our key insight is that using the diffusion model can improve the RL performance by constraining its exploration to high-value state-action regions. *We find our method is especially useful for the evader to learn escaping behaviors in the*

*All authors are associated with the Institute of Robotics and Intelligent Machines (IRIM), Georgia Institute of Technology, Atlanta, GA 30308, USA.

Correspondance Author: Zixuan Wu zwu380@gatech.edu

¹Code and implementation details are at <https://github.com/CORE-Robotics-Lab/Opponent-Modeling>

large multi-agent, multi-goal partially observable settings — Prisoner Escape and Narco Interdiction Domain (see §III-B). Increasing understanding of potential evader strategies will help future development of countermeasures.

Contributions: In summary, our contributions are three-fold:

- 1) Our work is the first to create a learning-based framework for evaders in large partially observable environments that learns without expert domain knowledge.
- 2) We propose a novel hierarchical system consisting of a diffusion model as a high level global path planner and a low level RL agent to learn evasive maneuvers, which significantly outperforms all baselines.
- 3) To the best of our knowledge, we pioneer the use of task-oriented costmap construction to enhance explainability, predictability, and flexibility, thereby facilitating a deeper understanding of the evader’s performance.

II. RELATED WORK

A. Pursuit-Evasion Games

A perfect information PEG (i.e., full observability) can be modeled as a differential game and solved using control theory [26]–[29]. In comparison, the incomplete information PEG (i.e., partial observability) is a more realistic setting. Researchers commonly use probabilistic models [30], [31] and formulate PEG as optimization problems with the objective of maximizing the payoff [32], [33]. Therefore, recent research also focuses on deriving the optimal policy via RL [32], [34], [35]. Unfortunately, most of RL work focuses on pursuit policies [32], [34], [36]. While Generative Adversarial Imitation Learning has been employed for training an evader policy, this approach requires a dataset showing expert evasive behaviors and a complex curriculum RL scheme [35]. Furthermore, prior work only validates this approach on a small map. In comparison, our method trains evasive RL policy from scratch without any evasion behavior demonstrations and is simpler and more suitable for large, adversarial, and partially observable domains.

B. Diffusion Models in Path Generating

Diffusion models are a class of generative models that have demonstrated impressive performance in generating sequential data across several applications, such as image synthesis and video generation [37]–[39]. Recently, there have been several works employing diffusion models in trajectory generation tasks. Diffuser [40] trains a diffusion model for trajectory generation on offline datasets and plans future trajectories with guided sampling. Diffusion policy extended this work to imitation learning and was able to learn robust policies for various pushing tasks conditioned only on visual inputs [41]. Recent work [15] has extended these approaches for generating trajectories of multiple opponents. There have also been many following works using diffusion models to synthesize trajectories and augment experience buffer for efficient offline RL training [42], [43]. However, these works only function in fully-observable domains, where building a world model is feasible. We instead use the diffusion model as a trajectory planner that allows the

reinforcement learning agent to generate diverse plan options in our partially observable pursuit-evasion domain.

C. Reinforcement Learning in Motion Planning

Recent works have demonstrated the success of RL for motion planning problems in dynamic environments [17], [44]–[47]. Many papers discuss how to use RL to avoid obstacles by analyzing exteroceptive sensor information such as RGB cameras [44], [47], LIDARs [46], [47], or laser data converted from images [45]. However, none of these prior works assumes the an adversarial environment, where the “obstacles” are intelligent pursuers, and the map size is as large as in our scenario.

The most similar work from the system design perspective is from [17] which also employs a hierarchical structure in goal-conditioned planning. However, their environment does not incorporate adversaries or multiple goals. Additionally, they require expert datasets for training their RL policy. Dynamic obstacles are considered in [48]; however, these obstacles can only run on a pre-defined segment with a constant velocity, and all the environment objects are observable such that A* search can be employed effectively. In our scenario, we assume the cameras are unobservable to the evader, while the pursuit team can leverage these cameras to detect and track the evader. Therefore, we use a diffusion model to generate diverse global candidate paths and make it possible for RL to do useful exploration about the map.

III. ENVIRONMENT

A. Partially Observable Markov Decision Process

We model adversarial search and tracking as a Partially Observable Markov Decision Process (POMDP). A POMDP for an agent can be defined by a state s , private observation o , action a , a transition function $\mathcal{T} : s \times a \mapsto s$. At each timestep t , an agent receives an observation o^t , chooses an action $a^t \in \mathcal{A}$, and obtains a reward $r^t : s \times a_i \mapsto \mathbb{R}$. The initial world state is drawn from a prior distribution ρ . In our environment (see §III-B), we assume the evader starts from a random position from in a corner region of the map while the pursuit team starts from a random position on the map.

B. Prisoner Escape and Narco Interdiction Domains

In our evaluation of the proposed algorithm, we adjust two large-scale pursuit-evasion domains from prior work [14] named Prisoner Escape and Narco Interdiction (Figure 2). In both domains, an evader (prisoner or smuggler) is being tracked by a team of search agents in a partially observable environment. We draw three hideouts each episodes from all the candidate hideouts. The game-ending goal of the evader is to reach any hideout on the map (considered as success), or reach the time limit (considered as failure). The heterogeneous pursuit team consists of static (cameras) and dynamic agents (search parties and helicopters) that collaborate to search and track the evader in both domains.

The maximum speed of the evader is always lower than the pursuit agents, making it crucial for the evader to plan evasive maneuvers to successfully reach the hideouts undetected.

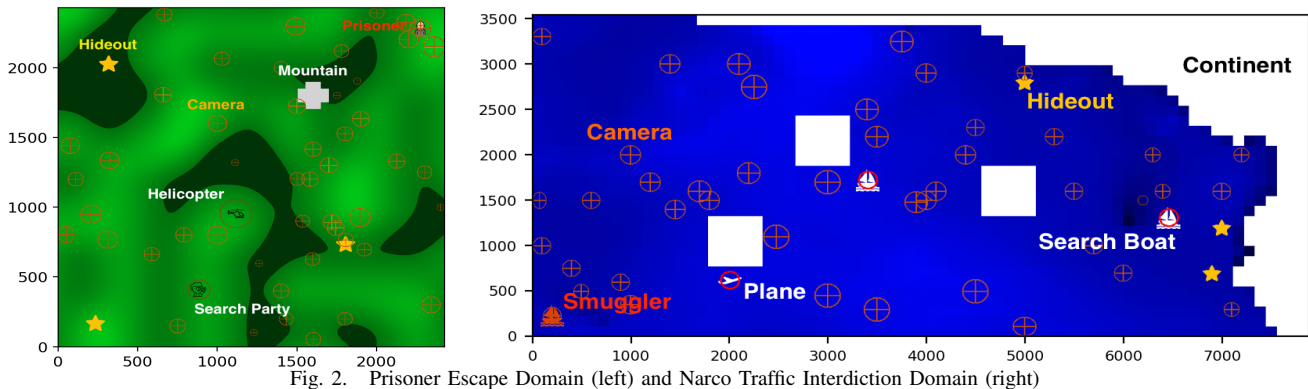


Fig. 2. Prisoner Escape Domain (left) and Narco Traffic Interdiction Domain (right)

The observation of the evader includes the current timestep, hideout locations, mountain locations, pursuer states and evader states. However, the camera locations and visibility map are hidden to the evader. These domains increase the complexity of the task and more closely match real-world dynamics compared to other pursuit-evasion games.

C. Pursuit Team Behavior

We create a heuristic policy for tracking the evader inspired by previous object searching works [49], [50] and the fact that pursuit teams typically follow some routine patterns. The search agents can choose to either 1) go to the last known location of the evader, 2) intercept the evader, or 3) search in the vicinity of the evader’s last known location. We assume the detection range of searching team d_s is parameterized by the agent type β_{type} , visibility c_v and evader speed s_e : $d_s = \alpha \cdot (\beta_{type} \cdot c_v \cdot s_e + \eta)$, which means a higher visibility and evader speed will lead to higher detection range. The pursuer policy is designed to effectively utilize the available information and adapt to a wide variety of different scenarios.

IV. METHOD

The evader’s objective is to reach one of the hideouts on the map and evade detection by the pursuit team, using only partial map knowledge and lacking any information about camera locations or models for whether the pursuers are able to detect the evader. RL or diffusion-based motion planning each partially fits our setting: RL can hypothetically learn to evade through trial-and-error. However, RL has difficulties with exploration in the large, adversarial, and multi-goal domains. On the other hand, diffusion-based motion planning can generate diverse plans that reach the goals; however, diffusion models struggle to learn evasive behaviors and avoid the pursuing agents. This weakness is due to the diffusion model is trained with a denoising loss objective that is not readily incorporated into RL [51]. Additionally, the partial observability induces high variance in training.

We propose to reap the benefits of both methods by leveraging diffusion models to guide RL exploration during training and generate path candidates at inference. We break down the hierarchy into the following: learning diffusion-based global plans that meet start, terminal, and obstacle constraints from RRT* paths (§IV-A), employing RL local evasive behaviors to avoid detection on route (§IV-B), and

path selection from reversely constructed costmap during inference (§IV-C).

A. Diffusion Based Global Plan

In this section, we describe how we leverage diffusion models as a generative motion planner to provide a prior for the RL agent to traverse in large, partially observable, and adversarial environments [52]. Since A* cannot generate the optimal path to guide RL exploration on partially observable maps with adversarial agents [53], we utilize a diffusion model to plan waypoints for an approximate path that the agent should follow. By using the diffusion model, our method is sample-time efficient and enables the downstream reinforcement learning algorithm to outperform prior approaches. The underlying insight is to produce diverse options from the diffusion model for global exploration to deal with map uncertainty.

The diffusion path planning should have three key attributes: 1) global constraints are satisfied (start and terminal locations, obstacles etc.); 2) generated plans are diverse and multimodal and 3) the sampling time of the diffusion model is low. We guide the diffusion sampling procedure using constraint guidance [15] to best satisfy the constraints and use a small number of sampling timesteps to keep the sampling time low. This low sampling time allows us to run the diffusion model during the RL training procedure which is difficult for traditional planners (e.g., RRT* and A*). Additionally, the parallel sampling at inference time provides diverse candidates for the agent to use.

We outline the diffusion training process in Algorithm 1. We first generate paths with RRT* (Line 3) — a sample-based motion planner that yields varied paths even for the same initial and target states, which enables the diffusion model to similarly generate diverse paths. Then we uniformly downsample the path into sparse waypoints (Line 4) and train a diffusion model based on these waypoints (Line 6-10). This process differs from Carvalho et al. [19], which trains a diffusion model directly from the dense and smoothed paths. Generating a path with a few waypoints is sufficient enough to act as the high level planner as we expect the RL policy to act as the low-level dynamic actor to move between waypoints. Generating fewer waypoints also allows sampling time to be faster, which is crucial for training in an RL loop.

The sampling process is similar to our previous work [15]

Algorithm 1: Diffusion Model Training

Data: Start Location \mathcal{S} , Goal Locations \mathcal{G} , Obstacle Location \mathcal{M} , Constraints $\mathcal{C} = \langle \mathcal{S}, \mathcal{G}, \mathcal{M} \rangle$, Data buffer \mathcal{D} , Noise Scheduling Terms $\alpha_i, \bar{\alpha}_i$, Learning Rate α , Denoising Timesteps T

Result: Diffusion Model s_θ

- 1 **while** buffer \mathcal{D} not full **do**
- 2 $c = \langle p_s, p_g, m \rangle \sim \mathcal{C}$; \triangleleft Draw global constraints
- 3 $\tau \leftarrow \text{RRT}^*(c)$; \triangleleft Plan RRT* path
- 4 $\tau \leftarrow \text{Sample}_\downarrow(\tau)$; \triangleleft Uniformly downsample path
- 5 $\mathcal{D} \leftarrow \tau, c$; \triangleleft Store trajectory, constrains in dataset
- 6 **while** not converged **do**
- 7 \triangleleft Draw τ, c diffusion timestep, and random noise
- 7 $\tau_0, c \sim \mathcal{D}$ $i \sim \mathcal{U}(1, T)$, $\epsilon \sim \mathcal{N}(0, I)$;
- 7 \triangleleft Compute Score Matching MSE Loss
- 8 $\tau_i \leftarrow \sqrt{\bar{\alpha}_i} \tau_0 + \sqrt{1 - \bar{\alpha}_i} \epsilon$;
- 9 $\mathcal{L}(\theta) = \|\epsilon - s_\theta(\tau_i, i, c)\|_2^2$;
- 9 \triangleleft Update Model
- 10 $\theta = \theta + \alpha \nabla_\theta \mathcal{L}(\theta)$

Algorithm 2: Diffusion Path Generator π^d

Data: Constraints \mathcal{C}

Result: Global plan τ^0

- 1 **while** τ^0 not satisfies constraints \mathcal{C} **do**
- 2 $\tau^T \leftarrow$ sample from $\mathcal{N}(0, I)$; \triangleleft Gaussian Noise
- 3 **for** all i from T to 1 **do**
- 4 $(\mu^i, \Sigma^i) \leftarrow s_\theta(\tau^i), \Sigma_\theta(\tau^i)$
- 5 $\tau^{i-1} \sim \mathcal{N}(\mu^i, \Sigma^i)$; \triangleleft Diffusion Denoise
- 6 $\tau^{i-1} \leftarrow \mathcal{C}(\tau^{i-1})$; \triangleleft Apply Constraints
- 7 **Return** τ^0

summarized in Algorithm 2 as diffusion path generator π^d . We apply global constraints at each denoising step (Line 6) to help generate a valid path from start to the end location.

B. RL Based Adversarial Behavior Learning

In addition to our diffusion model considering the global objectives, it is also important to design an algorithm directly interacting with the environment that can not only accomplish the tasks from the high-level planners but also capture the dynamic patterns in the map to achieve the local adversarial detection avoiding goals. Even the heuristics have been built in our previous works, we believe that a data-driven reinforcement learning algorithm is a more convenient way compared with the man-crafted policy and can perform better within a certain distribution.

Therefore we employ an RL algorithm Soft Actor-Critic (SAC) as the low-level policy with the following aims: 1) basically follow the waypoints from diffusion path and 2) learn to adjust its velocities to evade from searching agents. We summarize the RL training process in Algorithm 3 where we augment the observation with the current desired waypoint from the high-level planner (Line 2, 4). The training

Algorithm 3: Adversarial Behavior Learning

Data: Initial state s_0 , Diffusion Global Planner π^d , SAC replay buffer \mathcal{D}_s

Result: SAC low-level policy π^{l*}

- 1 **while** training episodes **do**
- 2 $\{w_i\}_{i=0}^{N_v} = \mathbf{w} \sim \pi^d(\mathbf{w}|s_0)$; \triangleleft Waypoints from π^d
- 3 **while** w_i not reached **do**
- 4 $O_{aug} \leftarrow [O|w_i]$; \triangleleft Concat current waypoint
- 5 $a \sim \pi^l(a|O_{aug})$; \triangleleft Action from low policy
- 6 $O'_{aug}, r \leftarrow \text{EnvStep}(a)$; \triangleleft Update env
- 7 $\mathcal{D}_s \leftarrow \{O_{aug}, a, O'_{aug}, r\}$; \triangleleft Push to buffer
- 8 **if** w_i reached **then**
- 9 $i \leftarrow i + 1$; \triangleleft Update to next waypoint
- 10 $\pi^{l*} \leftarrow \text{SAC}(\mathcal{D}_s)$; \triangleleft Update SAC parameters

objective can be formulated as Equation (1) where \approx means the similar low-level policy can be derived from both sides.

$$\begin{aligned} R &= \max_{\pi} \mathbb{E}_{\pi} \left[\sum_t \gamma^t \cdot r \right] \\ &\approx \max_{\pi^g} \mathbb{E}_{\pi^g} \left[\max_{\pi^l} \mathbb{E}_{\pi^l} \left[\sum_{\tau=0}^{t_g} \sum_{t=0}^{t_l} \gamma^t \cdot r \mid w^\tau \sim \pi^g(w|s^\tau) \right] \right] \\ &\approx \max_{\pi^l} \mathbb{E}_{\pi^l} \left[\sum_{\tau=0}^{t_g} \sum_{t=0}^{t_l} \gamma^t \cdot r \mid \mathbf{w} \sim \pi^d(\mathbf{w}|s_0), s_0 \sim \rho \right] \end{aligned} \quad (1)$$

ρ is the initial environment distribution for the start and hideout locations ($s_0 \sim \rho$ is omitted from the derivation), π^d is the diffusion global planner, and \mathbf{w} is the generated waypoints to be tracked, t_g is the number of waypoints. This equation shows that we are able to decompose our adversarial evading learning problem into a sequential optimization problem, including a waypoint generator and a low-level waypoint tracker, both of which aim to maximize the discounted accumulative reward. However, the unconstrained random exploration of these policies will subject to high variance from the partial observability, therefore we confine our exploration in a more reasonable region described by the diffusion policy distribution in the previous section. We set reward terms to guide the evader to reach the waypoint and avoid detection in Equation (2) where r_g is the reward given when reaching the waypoint, r_{adv} is the detection penalty, and r_d is the distance penalty to the next waypoint.

$$r = r_g + r_d + r_{adv} \quad (2)$$

C. Cost Map Construction and Inference

Even though we assume that the cameras and the terrain map information is totally unobservable for the evasive agent, we may know that there are some relations between the detection and these parts on the map. For example, the agent is easier to capture around the camera and more difficult to capture in the low visibility region. Therefore, it is possible

TABLE I
DIFFUSION-RL BENCHMARKS (MEAN \pm STD)

Domain	Prisoner Escape			Narco Interdiction		
	Score \uparrow	Detection \downarrow	Goal-Reach. \uparrow	Score \uparrow	Detection \downarrow	Goal-Reach. \uparrow
Non-Learning Approaches						
A-Star Heuristic	0.721 \pm 0.189	0.344 \pm 0.238	0.980 \pm 0.140	0.635 \pm 0.295	0.392 \pm 0.305	0.800 \pm 0.400
RRT-Star Heuristic	0.731 \pm 0.176	0.321 \pm 0.220	0.940 \pm 0.237	0.655 \pm 0.308	0.375 \pm 0.319	0.830 \pm 0.376
VO-Heuristic	0.738 \pm 0.113	0.323 \pm 0.143	0.980 \pm 0.140	0.635 \pm 0.099	0.426 \pm 0.116	1.000 \pm 0.000
Learning Approaches						
DDPG	0.234 \pm 0.342	0.725 \pm 0.404	0.070 \pm 0.255	0.305 \pm 0.321	0.645 \pm 0.374	0.000 \pm 0.000
SAC	0.779 \pm 0.117	0.058 \pm 0.108	0.130 \pm 0.336	0.486 \pm 0.347	0.434 \pm 0.406	0.010 \pm 0.099
Diffusion Only	0.779 \pm 0.092	0.276 \pm 0.116	1.000 \pm 0.000	0.776 \pm 0.127	0.261 \pm 0.148	1.000 \pm 0.000
Our Approaches						
Diffusion-RL [ours]	0.899 \pm 0.087	0.116 \pm 0.095	0.960 \pm 0.196	0.886 \pm 0.106	0.123 \pm 0.102	0.940 \pm 0.237
Diffusion-RL-Map [ours]	0.941\pm0.079	0.068 \pm 0.080	0.980 \pm 0.140	0.943\pm0.069	0.066 \pm 0.080	1.000 \pm 0.000

for us to spatially show detection risks on a posterior task-oriented cost map associated with the policies we derived as a reverse engineering problem.

Algorithm 4 describes our procedure. We run a certain number of episodes after the hierarchy is trained well (Line 1) and simultaneously record the evader location \mathbf{X} and its distance to the closest searching agent \mathbf{d} (Line 2). Then we select out the evader locations x_i with which the associated distance, d_i , is below a risk threshold ϵ and add a Gaussian distribution whose mean is x_i and standard deviation σ (Line 3-5). Next, we perform normalization and output the map.

Importantly, end-users can preview the global paths before execution or revise the cost map with the newly added global information, which adds more flexibility and explainability compared with traditional fully MDP based RL algorithms (Line 6). Finally we can select the global path with lowest cost based on the costmap in the inference (Line 7-8).

Algorithm 4: Costmap and Inference

Data: Initial state s_0 , Diffusion Global Planner π^d ,
Learned local policy π^{l*} , Costmap \mathbf{G} , Evasive agent location \mathbf{x}

Result: Selected global plan \mathbf{w}^*

```

1 while costmap constructing episodes do
2    $\mathbf{x}, \mathbf{d} = \text{Env}(s_0, \pi^d, \pi^{l*})$ 
3   for all  $x_i, d_i$  from  $\mathbf{x}, \mathbf{d}$  do
4     if  $d_i < \epsilon$  then
5        $\mathbf{G} \leftarrow \mathbf{G} + \mathcal{N}(x_i, \sigma^2)$ ;  $\triangleleft$  Add a Gaussian
6      $\mathbf{G} \leftarrow \text{adjust}(\mathbf{G}/\mathbf{G}_{max})$ ;
7      $\mathcal{T} \leftarrow \{\mathbf{w}_i : \mathbf{w}_i \sim \pi^d(\mathbf{w}|s_0)\}_{i=0}^{N_s}$ ;
8      $\mathbf{w}^* = \arg \max_{\mathbf{w}_i \in \mathcal{T}} \int_{\mathbf{w}_i} \mathbf{G}(w) dw$ ;

```

V. RESULTS & DISCUSSION

In this section, we will first benchmark our diffusion-RL framework against both heuristics and learning based

baselines. Then we visualize our constructed costmap which can help explain the results and show more advantages of our method. Then we justify our use of the diffusion model as the path generator. Next we validate our hierarchy in the real robot testbed. Finally we include a result discussion section.

A. Achieving Long-Term Planning and Short-Term Evasion

We propose to use the following metrics to quantitatively evaluate our method and compare it against the baselines: detection, goal-reaching rate, and score (\uparrow means higher is better and \downarrow means lower is better in Table I). Detection is the average number of steps when the evader is detected for each episode. Goal-reaching rate is the number of episodes in which the evader reach the goal in the time limit divided by the total number of episodes tested. The score metric is a weighted reward term that balances the aforementioned two main objectives in our domains: reaching the goal (± 50) and staying undetected by the opposing blue agents (-1 for each detection). Each metric is normalized by the min-max value of each category and we test the algorithms in 100 episodes with different random seeds from the training.

We compare our diffusion+RL method with learning based and non-learning based baselines. A* and RRT* heuristics are from our previous works [14] where the evader follows the A* or RRT* path and show some pre-scripted adversarial behaviors (e.g. heading to dense forest, changing velocity etc.) when the search team is nearby. Velocity obstacle (VO) method is widely used in the dynamic obstacle avoidance tasks which samples a velocity from the collision free velocity space [54]. From Table I, we find these heuristics can reach the goal at a high rate, but can be detected by the search team much more than our methods which leads to a lower score. The main reason is that the evader will be exposed to the unobservable cameras, which may attract the dynamic search team and the man-crafted evasive heuristic is not optimal for escaping. In comparison our approach, which utilizes the diffusion model as a motion planning module for a reinforcement learning agent, outperforms all non-learning baselines in terms of score and enables the agent to remain mostly undetected by the searching team while reaching the hideout (Table I).

Even though the reinforcement learning (DDPG & SAC) approaches directly optimize the score as their reward func-

tion, our methods outperform them on average by 109% on the score metric across both domains. At the same time, we find the goal reaching rate of the DDPG and SAC only methods are very low in prisoner escape domain (7%, 13%) and even lower in narco interdiction domain (0%, 1%). Interestingly, the SAC can outperform the DDPG in each metric we have across the two domains, which meets our expectation that SAC has more exploration ability from its stochastic policy and entropy regularization.

The SAC evader can be detected less than our map-based diffusion-RL algorithm by 19.12%, which is interesting and a red herring. Figure 3 shows a red colorbar for the distance between the evader and the closest agent in the pursuit team, and the diamond purple line indicates the diffusion planned global path. From the trajectory, we can see the SAC algorithm will lead the evader to the edge of the map where there is no camera but not the goal hideout. Instead, our method can loosely follow the diffusion waypoints (purple diamond) and simultaneously deviate a little to avoid the search team when they are close (indicated by magnet and orange dashed box). In addition, our method learns to reduce the evader speed when evading, which lowers the probability of detection, but maintains a higher speed when safer.

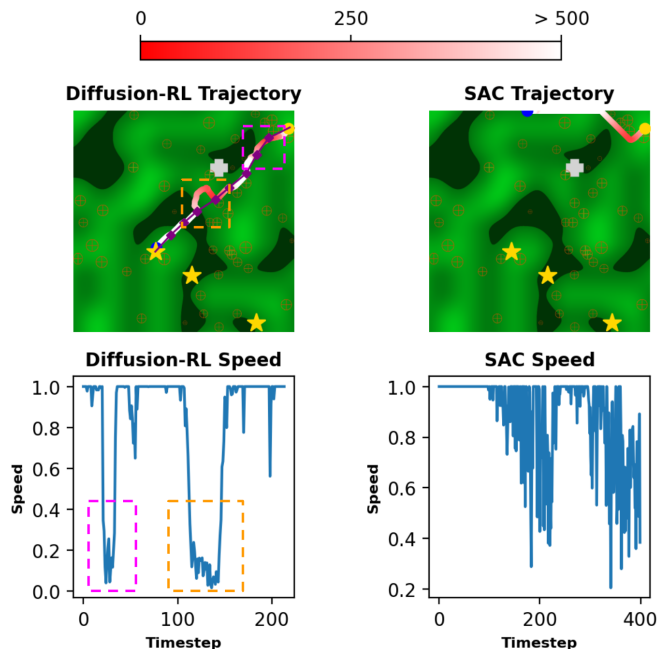


Fig. 3. Our Diffusion-RL trajectory vs SAC trajectory. Colorbar indicates distance between evader and closest pursuer and purple line indicates the diffusion global path. We find that our method (left) is able to evade the pursuers by deviating and decreasing the agent speed to reduce detection chance while still being able to reach the goal. On the contrary, the SAC policy is unable to reach the goal and only randomly changes its velocity.

B. Costmap

As discussed in §IV-C, we build a costmap based on the distance between evader and pursuer which implies detection risks. The costmap serves as an interpretable and memory efficient way to allow our RL agent to plan based on past experiences. Figure 4a shows the costmap, where the high intensity region indicates the evader is close to the search

team which may lead to a detection. We also find that the potential detection usually happens around the cameras (see Figure 4b), which is reasonable since the searching team will search the region after the evader is detected by the camera. Therefore, Figure 4c shows the evasive agent can select the best global path which receives lowest cost that can best conceal it from the camera array. At the inference stage, we can adjust the costmap with the new information we received. For example, we can add an undesired danger zone for the evader on the costmap (see Figure 4d) such that it will select another way to reach another hideout which will avoid the danger zone but potentially incurring more detection (see Figure 4e). We ablate our model with and without the costmap and show that the detection from map based path selection is further decreased by a half.

C. Diffusion Paths Validation

The learned diffusion model should be able to generate diverse global paths that satisfy start and terminal constraints such that it can guide the low-level RL to explore high-valued state spaces. Additionally, the diffusion model should be sample-time efficient to accelerate RL training and inference. Figure 5a-5b compares the diffusion global paths trained on the datasets from RRT* and another commonly used path planner A*. We see the diffusion model encodes a more diverse distribution of the paths leading to the final hideouts when using RRT*. Figure 5c and Table 5d shows the planning time for both the diffusion and RRT* algorithms. The diffusion model takes 85.7% less time generating one trajectory compared with RRT*, which requires a map search. Furthermore, the difference is enlarged when planning more paths since we can draw samples from diffusion model in parallel. We generate the results using a machine with 11th Gen Intel Core i9 processor and GeForce GTX 1660 Ti graphic card.

D. Real Robot Demonstration

We also test our method with the Robotarium [55] testbed to validate our method with real robot dynamics. Figure 6 shows the comparison between the RRT* heuristic and our method. We find the evader (red trajectory) equipped with our policy can reach the hideout and remain untracked by the searching team (blue and cyan trajectories) but the RRT* heuristic travels in a path with more cameras and is tracked by helicopter from $t \approx 90$. The result indicates that our data-driven learning based method can outperform the heuristics from the multi-agent interaction and map optimizations.

E. Discussion

The significant disparity in goal-reaching rates between RL alone and our approaches indicates that RL struggles with long-horizon exploration in our domain, supporting our premise in §I that diffusion models can guide RL exploration. Additionally, Figure 3 reveals that SAC can become trapped in a local minimum. From this, we infer that our methods can achieve long-term planning by providing the RL agent with a diffusion-based global plan while retaining the agility to

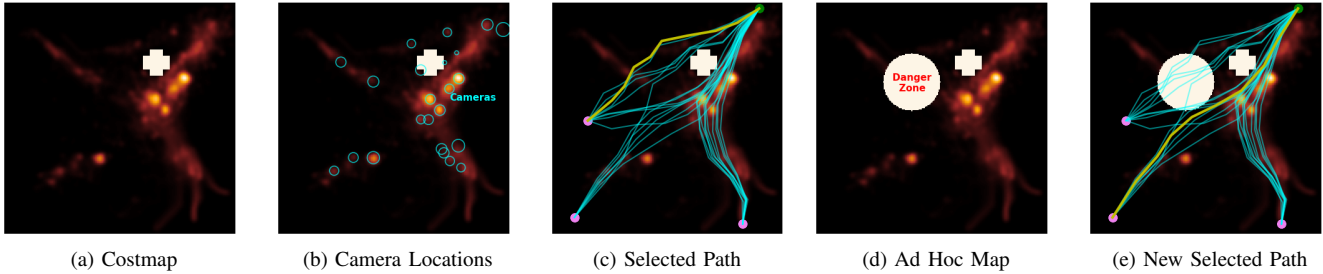
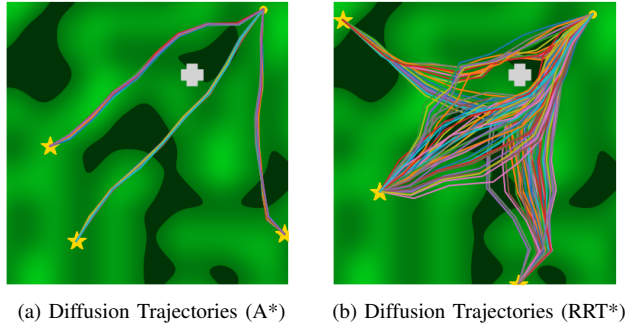
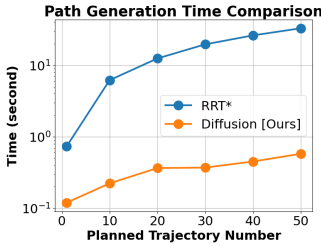


Fig. 4. Path Planning with the Costmap: The costmap (a) is constructed by correlating the agent’s risk of detection to its location on the map. We show in (b) that the agent is able to successfully identify where the cameras are. Given this costmap, the agent can select a path that best evades high cost regions (c). Additional obstacles can be added ad-hoc (d) and a new path can be chosen (e). The grey areas indicate untraversable obstacles or danger zones.



(a) Diffusion Trajectories (A*) (b) Diffusion Trajectories (RRT*)



Traj.	RRT*	Diffusion
1	0.7±0.2	0.1±0.0
10	6.2±0.3	0.2±0.0
20	12.5±0.6	0.4±0.1
30	19.7±1.5	0.4±0.0
40	26.3±1.9	0.5±0.0
50	33.0±2.3	0.6±0.2

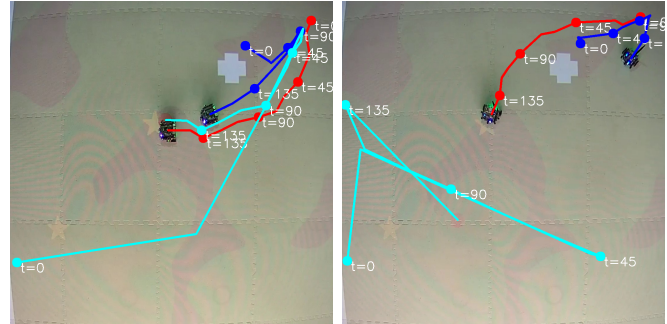
(c) Time Comparison (d) Time Comparison (mean±std)

Fig. 5. The paths from the diffusion model trained on RRT* are more diverse than those trained on A* (5a-5b). Additionally, compared to the traditional RRT* planner, the diffusion model leverages the power of parallel computing to generate trajectories an order of magnitude faster (5c-5d).

evade opponent agents in the short horizon. The cost map and time ablations in §V-B to §V-C demonstrate that our diffusion model can generate diverse samples and aid in downstream tasks such as cost map construction and path selection.

VI. CONCLUSION AND FUTURE WORK

In conclusion, we have presented a novel learning-based framework for evaders in large, partially observable, multi-agent pursuit-evasion settings. Our approach can help the evader reach the hideout and best conceal itself from capturing by using a hierarchy with a high-level diffusion path planner and a low-level RL evasive policy. Our work can also be extended to more general navigation problems (e.g. visual navigation, manipulator grasping etc.). However, our learned hierarchy requires additional interactions with the environments when constructing the costmap. In the future, we plan to integrate the map construction process into the RL training loop by iterating a location-only based value function $V(s)$ with the Bellman equation. Additionally, we will train the RL policy for both the pursuit and evasion sides



(a) RRT* Heuristic (b) Diffusion-RL-Map (ours)

Fig. 6. Pursuit-evasion trajectories: the evader, search party and helicopter trajectory are indicated with red, blue and cyan respectively. Evader is tracked from $t \approx 90$ with the RRT* heuristic but can escape from searching team with our method along the path to the hideout.

simultaneously and investigate the relationship between the Nash equilibrium with respect to team composition.

REFERENCES

- [1] R. Vidal, O. Shakernia, H. J. Kim, D. H. Shim, and S. Sastry, “Probabilistic pursuit-evasion games: theory, implementation, and experimental evaluation,” *IEEE transactions on robotics and automation*, vol. 18, no. 5, pp. 662–669, 2002.
- [2] W. Silkman, “The use of us naval surface combatants in the maritime counter narcotics interdiction effort: A major impact on the flow of drugs,” *Newport, Rhode Island, United States. Retrieved from Naval War College*, 2001.
- [3] Y. A. Hasan, A. Garg, S. Sugaya, and L. Tapia, “Defensive escort teams for navigation in crowds via multi-agent deep reinforcement learning,” *IEEE Robotics and Automation Letters*, vol. 5, no. 4, pp. 5645–5652, 2020.
- [4] E. Antonioni, V. Suriani, F. Riccio, and D. Nardi, “Game strategies for physical robot soccer players: A survey,” *IEEE Transactions on Games*, vol. 13, no. 4, pp. 342–357, 2021.
- [5] A. Afzalov, A. Lotfi, B. Inden, and M. E. Aydin, “A strategy-based algorithm for moving targets in an environment with multiple agents,” *SN Computer Science*, vol. 3, no. 6, p. 435, 2022.
- [6] V. Bulitko and N. Sturtevant, “State abstraction for real-time moving target pursuit: A pilot study,” in *AAAI Workshop: Learning For Search*. Citeseer, 2006, pp. 72–79.
- [7] A. I. A. Isaza, J. Lu, V. Bulitko, and R. Greiner, “A cover-based approach to multi-agent moving target pursuit,” in *Proceedings of the AAAI Conference on Artificial Intelligence and Interactive Digital Entertainment*, vol. 4, no. 1, 2008, pp. 54–59.
- [8] D. Sigurdson, V. Bulitko, W. Yeoh, C. Hernández, and S. Koenig, “Multi-agent pathfinding with real-time heuristic search,” in *2018 IEEE Conference on Computational Intelligence and Games (CIG)*. IEEE, 2018, pp. 1–8.
- [9] J. Kennedy and R. Eberhart, “Particle swarm optimization,” in *Proceedings of ICNN’95-international conference on neural networks*, vol. 4. IEEE, 1995, pp. 1942–1948.

- [10] Q. Liu, W. Wei, H. Yuan, Z.-H. Zhan, and Y. Li, "Topology selection for particle swarm optimization," *Information Sciences*, vol. 363, pp. 154–173, 2016.
- [11] Y. Bar-Shalom and X.-R. Li, *Multitarget-multisensor tracking: principles and techniques*. YBs Storrs, CT, 1995, vol. 19.
- [12] S. Jin and Z. Qu, "Pursuit-evasion games with multi-pursuer vs. one fast evader," in *2010 8th World Congress on Intelligent Control and Automation*, 2010, pp. 3184–3189.
- [13] J. Selvakumar and E. Bakolas, "Evasion with terminal constraints from a group of pursuers using a matrix game formulation," in *2017 American Control Conference (ACC)*. IEEE, 2017, pp. 1604–1609.
- [14] S. Ye, M. Natarajan, Z. Wu, R. Paleja, L. Chen, and M. C. Gombolay, "Learning models of adversarial agent behavior under partial observability," 2023.
- [15] S. Ye, M. Natarajan, Z. Wu, and M. Gombolay, "Diffusion based multi-agent adversarial tracking," *arXiv preprint arXiv:2307.06244*, 2023.
- [16] Z. Wu, S. Ye, M. Natarajan, L. Chen, R. Paleja, and M. C. Gombolay, "Adversarial search and tracking with multiagent reinforcement learning in sparsely observable environment," 2023.
- [17] J. Li, C. Tang, M. Tomizuka, and W. Zhan, "Hierarchical planning through goal-conditioned offline reinforcement learning," *IEEE Robotics and Automation Letters*, vol. 7, no. 4, pp. 10216–10223, 2022.
- [18] J. Liu, M. Stamatopoulou, and D. Kanoulas, "Dipper: Diffusion-based 2d path planner applied on legged robots," *arXiv preprint arXiv:2310.07842*, 2023.
- [19] J. Carvalho, A. T. Le, M. Baierl, D. Koert, and J. Peters, "Motion planning diffusion: Learning and planning of robot motions with diffusion models," in *2023 IEEE/RSJ International Conference on Intelligent Robots and Systems (IROS)*. IEEE, 2023, pp. 1916–1923.
- [20] G. Wang, F. Wei, Y. Jiang, M. Zhao, K. Wang, and H. Qi, "A multi-uv maritime target search method for moving and invisible objects based on multi-agent deep reinforcement learning," *Sensors*, vol. 22, no. 21, p. 8562, 2022.
- [21] M. Andrychowicz, F. Wolski, A. Ray, J. Schneider, R. Fong, P. Welinder, B. McGrew, J. Tobin, O. Pieter Abbeel, and W. Zaremba, "Hindsight experience replay," *Advances in neural information processing systems*, vol. 30, 2017.
- [22] P.-L. Bacon, J. Harb, and D. Precup, "The option-critic architecture," in *Proceedings of the AAAI conference on artificial intelligence*, vol. 31, no. 1, 2017.
- [23] P. Zhang, X. Chen, L. Zhao, W. Xiong, T. Qin, and T.-Y. Liu, "Distributional reinforcement learning for multi-dimensional reward functions," 2021.
- [24] E. Prianto, M. Kim, J.-H. Park, J.-H. Bae, and J.-S. Kim, "Path planning for multi-arm manipulators using deep reinforcement learning: Soft actor-critic with hindsight experience replay," *Sensors*, vol. 20, no. 20, p. 5911, 2020.
- [25] S. Nasiriany, H. Liu, and Y. Zhu, "Augmenting reinforcement learning with behavior primitives for diverse manipulation tasks," in *2022 International Conference on Robotics and Automation (ICRA)*. IEEE, 2022, pp. 7477–7484.
- [26] P. Hungerländer, "Discrete-time dynamic noncooperative game theory," 2014.
- [27] R. Isaacs, *Differential games: a mathematical theory with applications to warfare and pursuit, control and optimization*. Courier Corporation, 1999.
- [28] M. Sani, B. Robu, and A. Hably, "Pursuit-evasion game for nonholonomic mobile robots with obstacle avoidance using nmpc," in *2020 28th Mediterranean conference on control and automation (MED)*. IEEE, 2020, pp. 978–983.
- [29] M. Salimi, "A pursuit-evasion game with hybrid system of dynamics," *Mathematical Methods in the Applied Sciences*, 2020.
- [30] Y. Feng, L. Dai, J. Gao, and G. Cheng, "Uncertain pursuit-evasion game," *soft computing*, vol. 24, pp. 2425–2429, 2020.
- [31] R. Vidal, O. Shakernia, H. Kim, D. Shim, and S. Sastry, "Probabilistic pursuit-evasion games: theory, implementation, and experimental evaluation," *IEEE Transactions on Robotics and Automation*, vol. 18, no. 5, pp. 662–669, 2002.
- [32] Y. Wang, L. Dong, and C. Sun, "Cooperative control for multi-player pursuit-evasion games with reinforcement learning," *Neurocomputing*, vol. 412, pp. 101–114, 2020.
- [33] J. Selvakumar and E. Bakolas, "Min-max q-learning for multi-player pursuit-evasion games," *Neurocomputing*, vol. 475, pp. 1–14, 2022.
- [34] R. Zhang, Q. Zong, X. Zhang, L. Dou, and B. Tian, "Game of drones: Multi-uav pursuit-evasion game with online motion planning by deep reinforcement learning," *IEEE Transactions on Neural Networks and Learning Systems*, 2022.
- [35] X. Qu, W. Gan, D. Song, and L. Zhou, "Pursuit-evasion game strategy of usv based on deep reinforcement learning in complex multi-obstacle environment," *Ocean Engineering*, vol. 273, p. 114016, 2023.
- [36] Z. Zhou and H. Xu, "Decentralized optimal large scale multi-player pursuit-evasion strategies: A mean field game approach with reinforcement learning," *Neurocomputing*, vol. 484, pp. 46–58, 2022.
- [37] P. Dhariwal and A. Nichol, "Diffusion models beat gans on image synthesis," *Advances in Neural Information Processing Systems*, vol. 34, pp. 8780–8794, 2021.
- [38] J. Ho, C. Saharia, W. Chan, D. J. Fleet, M. Norouzi, and T. Salimans, "Cascaded diffusion models for high fidelity image generation," *J. Mach. Learn. Res.*, vol. 23, no. 47, pp. 1–33, 2022.
- [39] F.-A. Croitoru, V. Hondru, R. T. Ionescu, and M. Shah, "Diffusion models in vision: A survey," *IEEE Transactions on Pattern Analysis and Machine Intelligence*, 2023.
- [40] M. Janner, Y. Du, J. Tenenbaum, and S. Levine, "Planning with diffusion for flexible behavior synthesis," in *International Conference on Machine Learning*, 2022.
- [41] C. Chi, S. Feng, Y. Du, Z. Xu, E. Cousineau, B. Burchfiel, and S. Song, "Diffusion policy: Visuomotor policy learning via action diffusion," in *Proceedings of Robotics: Science and Systems (RSS)*, 2023.
- [42] H. He, C. Bai, K. Xu, Z. Yang, W. Zhang, D. Wang, B. Zhao, and X. Li, "Diffusion model is an effective planner and data synthesizer for multi-task reinforcement learning," *Advances in Neural Information Processing Systems*, vol. 36, 2024.
- [43] Z. Ding, A. Zhang, Y. Tian, and Q. Zheng, "Diffusion world model," 2024.
- [44] Z. Xue and T. Gonsalves, "Vision based drone obstacle avoidance by deep reinforcement learning," *AI*, vol. 2, no. 3, pp. 366–380, 2021.
- [45] L. Gao, J. Ding, W. Liu, H. Piao, Y. Wang, X. Yang, and B. Yin, "A vision-based irregular obstacle avoidance framework via deep reinforcement learning," in *2021 IEEE/RSJ International Conference on Intelligent Robots and Systems (IROS)*. IEEE, 2021, pp. 9262–9269.
- [46] B. Rubí, B. Morcego, and R. Pérez, "Quadrotor path following and reactive obstacle avoidance with deep reinforcement learning," *Journal of Intelligent & Robotic Systems*, vol. 103, pp. 1–17, 2021.
- [47] R. Cimurs, J. H. Lee, and I. H. Suh, "Goal-oriented obstacle avoidance with deep reinforcement learning in continuous action space," *Electronics*, vol. 9, no. 3, p. 411, 2020.
- [48] L. Kästner, T. Buiyan, L. Jiao, T. A. Le, X. Zhao, Z. Shen, and J. Lambrecht, "Arena-rosnav: Towards deployment of deep-reinforcement-learning-based obstacle avoidance into conventional autonomous navigation systems," in *2021 IEEE/RSJ International Conference on Intelligent Robots and Systems (IROS)*. IEEE, 2021, pp. 6456–6463.
- [49] K. E. C. Booth, C. Piacentini, S. Bernardini, and J. C. Beck, "Target search on road networks with range-constrained uavs and ground-based mobile recharging vehicles," *IEEE Robotics and Automation Letters*, vol. 5, no. 4, pp. 6702–6709, 2020.
- [50] A. I. A. Isaza, J. Lu, V. Bulitko, and R. Greiner, "A cover-based approach to multi-agent moving target pursuit," in *Proceedings of the AAAI Conference on Artificial Intelligence and Interactive Digital Entertainment*, vol. 4, no. 1, 2008, pp. 54–59.
- [51] Z. Zhu, H. Zhao, H. He, Y. Zhong, S. Zhang, H. Guo, T. Chen, and W. Zhang, "Diffusion models for reinforcement learning: A survey," 2024.
- [52] Z. Wu, S. Ye, M. Natarajan, L. Chen, R. Paleja, and M. C. Gombolay, "Adversarial search and tracking with multiagent reinforcement learning in sparsely observable environment," in *2023 International Symposium on Multi-Robot and Multi-Agent Systems (MRS)*, 2023, pp. 43–49.
- [53] L. Kästner, T. Buiyan, L. Jiao, T. A. Le, X. Zhao, Z. Shen, and J. Lambrecht, "Arena-rosnav: Towards deployment of deep-reinforcement-learning-based obstacle avoidance into conventional autonomous navigation systems," in *2021 IEEE/RSJ International Conference on Intelligent Robots and Systems (IROS)*, 2021, pp. 6456–6463.
- [54] P. Fiorini and Z. Shiller, "Motion planning in dynamic environments using velocity obstacles," *The international journal of robotics research*, vol. 17, no. 7, pp. 760–772, 1998.
- [55] S. Wilson, P. Glotfelter, L. Wang, S. Mayya, G. Notomista, M. Mote, and M. Egerstedt, "The robotarium: Globally impactful opportunities,

challenges, and lessons learned in remote-access, distributed control of multirobot systems," *IEEE Control Systems Magazine*, vol. 40, no. 1, pp. 26–44, 2020.